On the Phase Structure of QCD in a Finite Volume

Jens Braun

Theoretisch-Physikalisches Institut, Friedrich-Schiller-Universität Jena, 07743 Jena, Germany

TRIUMF, 4004 Wesbrook Mall, Vancouver, BC V6T 2A3, Canada

Bertram Klein

Physik Department, Technische Universität München, James-Franck-Strasse 1, 85748 Garching, Germany

Bernd-Jochen Schaefer

Institut für Physik, Karl-Franzens-Universität, 8010 Graz, Austria

Institut für Theoretische Physik, Justus-Liebig-Universität Giessen, 35392 Giessen, Germany

Abstract

The chiral phase transition in QCD at finite chemical potential and temperature can be characterized for small chemical potential by its curvature and the transition temperature. The curvature is accessible to QCD lattice simulations, which are always performed at finite pion masses and in finite simulation volumes. We investigate the effect of a finite volume on the curvature of the chiral phase transition line. We use functional renormalization group methods with a two flavor quark-meson model to obtain the effective action in a finite volume, including both quark and meson fluctuation effects. Depending on the chosen boundary conditions and the pion mass, we find pronounced finite-volume effects. For periodic quark boundary conditions in spatial directions, we observe a *decrease* in the curvature in intermediate volume sizes, which we interpret in terms of finite-volume quark effects. Our results have implications for the phase structure of QCD in a finite volume, where the location of a possible critical endpoint might be shifted compared to the infinite-volume case.

Keywords: curvature, QCD, chiral phase transition, finite-volume effects

1. Introduction

An important theoretical method for the exploration of the QCD phase diagram at finite temperature and quark chemical potential is the simulation of the theory on a finite space-time lattice. While this approach is fully non-perturbative and incorporates most relevant physical effects, the price to be paid is a restriction to finite simulation volumes and to pion masses which only recently approach physical values [1]. In addition, the complex phase of the fermion determinant at finite quark chemical potential makes lattice simulations with Monte-Carlo methods for finite-density systems difficult.

Different strategies have been developed to cope with this sign problem in lattice QCD. For example, the partition function can be evaluated with re-weighting techniques [2, 3, 4] or Taylor-expanded around vanishing chemical potential [5, 6, 7, 8, 9, 10]. Alternatively, using an imaginary quark chemical potential for which no sign problem is present, the theory can be simulated at finite chemical potential, and the results can be continued to real values of the chemical potential [11, 12, 13]. The convergence of the Taylor-expansion method has been investigated e.g. in [10] and has recently been studied in an effective low-energy model [14, 15]. For a review of the state of lattice techniques see e.g. [16, 17, 18, 19].

Both approaches have been used to calculate the curvature of the QCD phase transition line in the temperature and baryon chemical potential plane, albeit for different values of the number of quark flavors, the size of the simulation volume and the pion mass [11, 12, 20, 21, 22, 23]. At present, the results from both approaches with different parameter values differ significantly, and our understanding of these results should be improved by a better grasp of the influence of these pa-

rameters.

In this context low-energy models of QCD are very useful to investigate the effects, e.g., of explicit chiral symmetry breaking or of a finite volume, and to provide a framework for understanding better the mechanisms of chiral symmetry breaking. Examples include NJL-type models and quark-meson-type models, see e. g. Refs. [24, 25, 26, 27, 28, 29, 30, 31, 32, 33, 34, 35, 36, 37, 38], as well as Polyakov-loop extended versions thereof, see e. g. Refs. [39, 40, 41, 42, 43, 44, 45, 46, 47, 48, 49, 50, 51, 52].

For the physics of such models in a finite volume, in addition to the fermionic fluctuations, the fluctuations of bosonic fields are of utmost importance [30, 53]. For a continuous symmetry such as the chiral flavor symmetry, bosonic fluctuations of Goldstone modes restore the symmetry in a finite-volume system in the absence of explicit symmetry breaking. Consequently, no phase with spontaneously broken chiral symmetry exists in the chiral limit. In order to capture the effects of long-range fluctuations, we use a functional renormalization group (RG) approach in the formulation according to Wetterich [54]. For reviews of and introductions to this functional RG approach we refer the reader to Refs. [55, 56, 57, 58, 59, 60, 61, 62, 63, 64, 65, 66]. This approach can also be adapted to a finite-volume system, see Refs. [30, 31, 32, 67, 68, 69, 53, 70].

When a system involving fermions is put into a finite Euclidean box, the anti-commutation relations demand anti-periodic boundary conditions for the fields in the Euclidean time direction. In contrast, the boundary conditions in spatial directions are not determined by a physical constraint, and one is free to choose either periodic or anti-periodic boundary conditions [71]. In lattice QCD simulations, often spatial periodic boundary conditions for the quark fields are chosen to minimize finite-volume effects. For small volume size, the presence of a resulting spatial zero-momentum mode for the quark fields can affect the formation of the chiral condensate. The choice of boundary condition leads to significant differences in the results for the condensate and the Goldstone spectrum [31] as well as for the transition temperature [32]. Contrary to naive expectations, contributions from the zero-mode can enhance the chiral condensate in a finite volume, while for either choice of boundary condition chiral symmetry is restored in the small-volume limit and ultimately the condensate vanishes [31]. A similar effect in the pion mass has been observed in Dyson-Schwinger equations [72].

As a consequence of this observation, we expect that the phase transition line at finite quark chemical potential and temperature will be affected by a finite volume. In NJL-type model calculations, the chiral condensate gives mass to constituent quarks, and an enhancement of the chiral condensate leads to a corresponding increase in the constituent quark mass. At finite quark chemical potential, more massive quarks lead to a decrease of the sensitivity of the system to changes in the quark chemical potential. Hence, we expect that the chiral transition temperature is less sensitive to the chemical potential and the curvature of the transition line in the μ-T–plane decreases for periodic spatial quark boundary conditions in those volume ranges where this effect pertains. In a recent contribution to proceedings [68], we have briefly reported on first results from an investigation of this hypothesis for values of the volume and the pion mass that are relevant for current lattice simulations. In this letter, we detail our studies on this question and present new results for the physical value of the pion mass. In addition, we employ a regularization scheme different from the one used in Ref. [68]. This constitutes a nontrivial check of our earlier results. As we shall discuss below, our new results do indeed confirm that the curvature of the chiral phase transition line has an intriguing dependence on the volume size.

In Sec. 2 we introduce the RG equations in a finite volume for a quark-meson model truncation. The results for the curvature of the phase-transition line at finite temperature and chemical potential are presented and discussed in Sec. 3. We summarize our results, draw conclusions and present an outlook in Sec. 4.

2. Renormalization Group Equations in a Finite Volume

We use for our investigation the quark-meson model in a finite volume. At the ultraviolet (UV) scale Λ, the model is defined by the bare effective action

$$\Gamma_\Lambda[\bar{q},q,\phi] = \int d^4x \Big\{ \frac{1}{2} Z_\phi (\partial_\mu \phi)^2 + U_\Lambda(\phi^2) - c\sigma \Big\} + \bar{q}\left(Z_\psi \mathrm{i}\partial\!\!\!/ + \mathrm{i}g(\sigma + i\vec{\tau}\cdot\vec{\pi}\gamma_5) + \mathrm{i}\gamma_0\mu \right) q \quad (1)$$

with $\phi^\mathrm{T} = (\sigma, \vec{\pi})$. The mesonic potential at the UV scale is parameterized by two couplings, m_Λ^2 and λ_Λ,

$$U_\Lambda(\phi^2) = \frac{1}{2} m_\Lambda^2 \phi^2 + \frac{1}{4} \lambda_\Lambda (\phi^2)^2 \,. \quad (2)$$

A current quark mass term $m_c \bar{q} q$ which explicitly breaks the chiral symmetry has been bosonized and leads to a term $-c\sigma$ linear in the radial σ field. The symmetry-breaking parameter c is related to the quark mass through a combination of the UV parameters.

In this work we study the RG flow of the effective action in leading order of the derivative expansion (LODE)[1], where a (possible) space dependence of the expectation value of the scalar fields is not taken into account and the wave-function renormalizations Z_ϕ and Z_ψ are considered to be constant, $Z_\phi \equiv 1$ and $Z_\psi \equiv 1$. At finite temperature, this implies that we also neglect a possible difference of the wave-function renormalizations parallel and perpendicular to the heat-bath [73]. These approximations should by no means be confused with a mean-field (large-N_c) approximation. On the contrary, the LODE already includes effects beyond the mean-field limit. A detailed discussion of the relation of the present approximation to the mean-field approximation in terms of a derivative expansion and a large-N_c expansion of the effective action can be found in Refs. [74, 73, 75]. In studies of the quark-meson model, however, the anomalous dimensions associated with Z_ϕ and Z_ψ are found to be small [26]. Therefore we believe that the LODE is already sufficient for this study.

For our derivation of the RG flow equations for the quark-meson model in a finite volume we use the Wetterich equation [54]

$$\partial_t \Gamma_k = \frac{1}{2}\mathrm{STr}\left\{\left[\Gamma_k^{(2)} + R_k\right]^{-1}(\partial_t R_k)\right\} . \tag{3}$$

For explicit calculations, we employ optimized regulator functions, see Refs. [76, 77]. For details on optimization of RG flows, we refer the reader to Refs. [78, 79, 80, 60]. At finite temperature and in a finite volume, the $3d$ regulator allows us to separate the finite-volume contributions from the finite-temperature contributions, which yields an exceptionally simple form for the RG flow equation. To be specific, we employ the following regulator functions for bosonic (B) and fermionic (F) fields:

$$\begin{aligned} R_\mathrm{B}(p_0, \vec{p}) &= \vec{p}^{\,2} r_\mathrm{B}(\vec{p}^{\,2}/k^2) \quad \text{and} \\ R_\mathrm{F}(p_0, \vec{p}) &= \not{p}\, r_\mathrm{F}(\vec{p}^{\,2}/k^2) . \end{aligned} \tag{4}$$

The shape functions $r_\mathrm{B}(x)$ and $r_\mathrm{F}(x)$ are given explicitly by

$$\begin{aligned} r_\mathrm{B}(x) &= \left(\frac{1}{x} - 1\right)\Theta(1-x) \quad \text{and} \\ r_\mathrm{F}(x) &= \left(\frac{1}{\sqrt{x}} - 1\right)\Theta(1-x) . \end{aligned} \tag{5}$$

In order to derive the RG flow equations for a system in a finite four-dimensional Euclidean volume $L^3 \times 1/T$ with temperature T, we replace each spatial momentum integral in the evaluation of the trace in Eq. (3) by a sum over discrete momenta:

$$\int_{-\infty}^{\infty} dp_i \to \frac{2\pi}{L}\sum_{n_i \in \mathbb{Z}} \quad ; \quad i = 1, 2, 3 . \tag{6}$$

While the boundary conditions in the Euclidean time direction are fixed by the statistics of the fields, we are free in the choice of the boundary conditions for the bosons and fermions in the spatial directions. In the following we use the short-hand notation

$$\vec{p}_\mathrm{p}^{\,2} = \frac{4\pi^2}{L^2}\sum_{i=1}^{3} n_i^2 \quad \text{and} \quad \vec{p}_\mathrm{a}^{\,2} = \frac{4\pi^2}{L^2}\sum_{i=1}^{3}\left(n_i + \frac{1}{2}\right)^2 \tag{7}$$

for the three-momenta in the case of periodic (p) and anti-periodic (a) boundary conditions. The flow equation for the effective potential of the quark-meson model in a finite cubic volume with length L at finite temperature T and quark chemical potential μ is then given by

$$\begin{aligned} \partial_t U_k(\phi^2) &= k^5\Bigg[\frac{3}{E_\pi}\left(\frac{1}{2} + n_B(E_\pi)\right)\mathcal{B}_\mathrm{p}(kL) \\ &\quad + \frac{1}{E_\sigma}\left(\frac{1}{2} + n_B(E_\sigma)\right)\mathcal{B}_\mathrm{p}(kL) \\ &\quad - \frac{2N_c N_f}{E_q}\Big(1 - n_F(E_q, \mu) \\ &\quad - n_F(E_q, -\mu)\Big)\mathcal{B}_\mathrm{l}(kL)\Bigg], \end{aligned} \tag{8}$$

where the first two terms correspond to contributions of the mesonic modes, and the last term with opposite overall sign corresponds to the quark contributions, see also Ref. [69]. The effective quasi-particles energies are given by

$$E_i = \sqrt{k^2 + M_i^2} , \quad i \in \{\pi, \sigma, q\} , \tag{9}$$

with the corresponding mesonic

$$M_\pi^2 = 2\frac{\partial U}{\partial \phi^2} , \qquad M_\sigma^2 = 2\frac{\partial U}{\partial \phi^2} + 4\phi^2\frac{\partial^2 U}{\partial(\phi^2)^2} \tag{10}$$

and squared quark masses

$$M_q^2 = g^2\phi^2 . \tag{11}$$

The usual bosonic and fermionic occupation numbers read

$$n_B(E) = \frac{1}{e^{E/T} - 1} , \quad n_F(E, \mu) = \frac{1}{e^{(E-\mu)/T} + 1} . \tag{12}$$

[1] This approximation is also known as the local potential approximation (LPA).

$m_\pi^{(0)}$ [MeV]	$f_\pi^{(0)}$ [MeV]	m_Λ [GeV]	λ_Λ	c [GeV^3]
100	90	1.003	100	9.02×10^{-4}
138	92	0.998	100	1.76×10^{-3}
200	97	0.982	100	3.88×10^{-3}

Table 1: Initial UV values for the RG calculation with $N_{\max} = 2$ for the three values of the pion mass considered in the main results. Here, $m_\pi^{(0)}$ is the pion mass in infinite volume for vanishing temperature and chemical potential, whereas $f_\pi^{(0)}$ denotes the respective value for the pion decay constant. We have fixed the parameters such that the values for $m_\pi^{(0)}$ and $f_\pi^{(0)}$ are consistent with chiral perturbation theory [83]. All results have been obtained with a UV cutoff $\Lambda = 1.5$ GeV and a constant Yukawa coupling $g = 3.258$.

The dependence on the finite spatial volumes is encoded in the mode counting functions $\mathcal{B}_\mathrm{l}$:

$$\mathcal{B}_\mathrm{l}(kL) = \frac{1}{(kL)^3} \sum_{\vec{n}\in\mathbb{Z}^3} \Theta\Big((kL)^2 - \vec{p}_\mathrm{l}^{\,2} L^2\Big) \,, \tag{13}$$

where $\mathrm{l} \in \{\mathrm{a}, \mathrm{p}\}$ and $\vec{n}$ labels the three-dimensional vector of integers. Depending on the choice for the spatial boundary conditions for the quarks, the appropriate function $\mathcal{B}_\mathrm{l}$ appears in the last term of Eq. (8). For small kL we find for periodic boundary conditions

$$\lim_{kL\to 0} \mathcal{B}_\mathrm{p}(kL) \sim \frac{1}{(kL)^3} \tag{14}$$

and for antiperiodic boundary conditions

$$\lim_{kL\to 0} \mathcal{B}_\mathrm{a}(kL) = 0 \,. \tag{15}$$

The behavior of $\mathcal{B}_\mathrm{p}$ for periodic spatial boundary conditions reflects the fact that the dynamics of the system for small kL is mainly governed by the spatial zero modes.

The flow equation (8) for the chiral order-parameter potential can be coupled straightforwardly to the confinement order-parameter potential, namely the Polyakov-loop potential. We give the flow equation including the dependence on the minimum of the Polyakov-loop potential in Appendix A. In the following, however, we will not consider such an extension in our numerical analysis but restrict ourselves to the flow equation (8). The possible consequences of this restriction are discussed in the conclusion, together with the implications of our results.

In the limit of infinite volume ($L \to \infty$) we find for both boundary conditions, $\mathrm{l} \in \{\mathrm{a}, \mathrm{p}\}$,

$$\lim_{kL\to\infty} \mathcal{B}_\mathrm{l}(kL) = \frac{1}{6\pi^2} \,. \tag{16}$$

As expected, in this limit the same flow equation for the effective potential for infinite volume is recovered which has been found with a similar regulator function for $L \to \infty$ in [29, 28, 35].

In order to solve the RG flow for the scale-dependent effective mesonic potential U_k, we expand the potential in a Taylor series in scale dependent local n-point couplings $a_{n,k}$ around its scale-dependent minimum $\sigma_{0,k}$

$$U_k(\phi^2) \quad = \quad \sum_{n=0}^{N_{\max}} \frac{a_{n,k}}{2^n n!} (\phi^2 - \sigma_{0,k}^2)^n . \tag{17}$$

Due to the presence of the symmetry-breaking term $-c\sigma$, the minimum is shifted from its value in the chiral limit. The condition

$$\frac{\partial}{\partial\sigma} U_k(\sigma^2 + \vec{\pi}^2)\bigg|_{\vec{\pi}=\vec{0},\sigma=\sigma_{0,k}} \stackrel{!}{=} c \tag{18}$$

ensures that the potential is always expanded around the actual physical minimum [67]. From Eq. (18) one sees that the RG flow of the coupling $a_{2,k} \equiv m_k^2$ and the minimum $\sigma_{0,k}$ are related by the simple condition

$$a_{2,k}\sigma_{0,k} = c \,. \tag{19}$$

This condition keeps the potential minimum at $(\sigma, \vec{\pi}) = (\sigma_{0,k}, \vec{0})$.

The RG flow equations for the couplings $a_{n,k}$ and $\sigma_{0,k}$ can be obtained by expanding the equation for the effective potential, Eq. (8), around the running minimum $\sigma_{0,k}$ and then projecting it onto the derivative of the ansatz, Eq. (17), with respect to k. In general, this procedure results in an infinite set of flow equations for all $a_{n,k}$. In order to obtain a finite set of flow equations, we truncate the Taylor series, Eq. (17), at a fixed order $N_{\max}$ and include thus fluctuations around the minimum up to order $2N_{\max}$ in the mesonic fields. The convergence of such an expansion in powers of the fields, i.e., in n-point functions, has been studied quantitatively in Ref. [81] at vanishing temperature by computing critical exponents and for the LODE at finite temperature in Ref. [82]. The resulting set of coupled first-order differential equations can then be solved numerically for example by standard Runge-Kutta methods.

In the following we use $N_{\max} = 2$ and fix the parameters $m_\Lambda^2 \equiv a_{1,\Lambda}$, $\lambda_\Lambda \equiv a_{2,\Lambda}/2$, c and g such that, at zero temperature and chemical potential, the values of the pion mass and the pion decay constant are consistent with chiral perturbation theory [83], see Tab. 1. While we consider the couplings m_Λ and λ_Λ to be RG-scale dependent, we keep the Yukawa coupling constant in the present study, $g = 3.258$. Together with the value of the pion decay constant, the Yukawa coupling then determines the constituent quark mass, see Eq. (11). Note that the four-boson coupling is marginal. For the UV cutoff Λ (initial RG scale), we choose $\Lambda = 1.5$ GeV. This scale can be interpreted as a hadronic mass scale below which hadronic operators are considered to be the relevant degrees of freedom and the dynamics are dominated by light pions. Of course, the precise values of the UV cutoff and the couplings are scheme-dependent. However, our main results are consistent with results that have been obtained using a different scheme, see Ref. [68] and the discussion below, provided that the parameters are chosen such that the values of the IR observables are identical.

3. The phase boundary in a finite volume

In the following we discuss finite-volume effects on the shape of the chiral QCD phase diagram at small chemical potentials. A very useful quantity for a description of the phase transition close to the temperature axis is the curvature κ of the transition line at $\mu = 0$, since it is accessible to both QCD lattice simulations and phenomenological models. It appears as the first non-vanishing coefficient in a Taylor series expansion of the transition line $T_\chi(\mu)$ in powers of μ^2 around vanishing chemical potential. It is defined according to

$$\frac{T_\chi(\mu, L, m_\pi^{(0)})}{T_\chi(\mu=0, L, m_\pi^{(0)})} = 1 - \kappa(L, m_\pi^{(0)}) \frac{\mu^2}{\pi^2 T_\chi^2(0, L, m_\pi^{(0)})} + \dots , \quad (20)$$

where $m_\pi^{(0)} = m_\pi(T = 0, \mu \to 0, L \to \infty)$ is the pion mass in infinite volume for vanishing temperature and chemical potential. Thus, the volume dependence of the phase diagram for small chemical potentials is encoded in the curvature κ which depends on L and $m_\pi^{(0)}$.

In Table 2, we list some results for the curvature κ obtained with different lattice methods. Only the result for $N_f = 2$ flavors from [11] could be compared directly to our calculations. The comparison between the different lattice results [21, 20] for $N_f = 3$ shows that the values differ significantly with a change of both the lattice current quark mass am_c and the simulation volume $L^3 \times 1/T$. We investigate the effect of the volume on the curvature to see if such an effect contributes to these differences.

Before we present our results for the volume dependence of κ, we briefly discuss its dependence on $m_\pi^{(0)}$ in infinite volume ($L \to \infty$).

In the chiral limit, results for the curvature in infinite volume have been obtained in Ref. [29] for the same model considered here. For a Taylor expansion of the effective potential, as in the present paper, to order ϕ^4 ($N_{\max} = 2$), a value $\kappa = 1.27$ has been found. This value is compatible with the results from the present calculation. In comparison, solving for the full effective potential on a grid, a value of $\kappa = 1.14$ has been obtained [29].

For finite pion masses, we show our results for the curvature in infinite volume $\kappa(L \to \infty, m_\pi^{(0)})$ in Tab. 3 as a function of the pion mass $m_\pi^{(0)}$. We observe that κ increases slightly with increasing pion mass. This behavior is in contrast to general expectations [84] and (lattice) gauge theory studies, where it was found that κ decreases with increasing m_π, i.e., increasing current quark mass m_c. This can be understood in terms of the constituent quark picture: The constituent quark mass m_q increases for increasing current quark mass m_c. Hence, the system becomes less sensitive to the chemical potential at any given value. Since the chiral phase temperature has only a weak dependence on m_c, the curvature $\kappa \sim T_\chi(0) d^2 T_\chi(\mu)/d\mu^2$ becomes smaller. While the first part of the argument holds for the quark-meson model as well, the chiral phase transition temperature has a comparatively strong dependence on m_c in model studies [26, 27, 29, 32]. This is in contrast to lattice studies, see e. g. Ref. [85]. Because the expansion parameter $\mu^2/T_\chi^2(0, L, m_\pi^{(0)})$ in our definition of the curvature is normalized with the transition temperature, this strong dependence also enters the coefficient κ. From the combination of both effects, we find that the resulting coefficient for the curvature increases slightly with increasing m_c.

In Figs. 1 and 2 we show our results for the relative change in the curvature $\Delta\kappa = (\kappa(L, m_\pi^{(0)}) - \kappa(\infty, m_\pi^{(0)}))/\kappa(\infty, m_\pi^{(0)})$ as a function of the volume size L and of the dimensionless quantity $m_\pi^{(0)} L$ for three different values of the pion mass $m_\pi^{(0)}$. For a given value of L, the black symbols represent the median values for $\Delta\kappa$ which have been obtained from fits to the transition curve $T_\chi(\mu)$ with polynomials to order μ^2, μ^4 and μ^6. The error bands for $\Delta\kappa$ (shaded areas) are also estimated from these fits. In addition, systematic truncation errors

method	ref.	N_f	am_c	$L^3 \times 1/T$	κ
imaginary μ	[11]	2	0.032	$8^3 \times 4$	0.500(54)
imaginary μ	[20]	3	0.026	$8^3 \times 4$	0.667(6)
Taylor series	[21]	3	0.005	$12^3 \times 4, 16^3 \times 4$	1.13(45)
Taylor series	[22]	2 + 1	[a]	$32^3 \times 8$	0.58(2)(4)
Taylor series	[23]	2 + 1	[a]	$24^3 \times 8, 28^3 \times 10$	0.59(18)[b]

[a] quark masses close to physical values, more than one value

[b] result from chiral condensate

Table 2: Results for the curvature κ from lattice simulations for $N_f = 2$, $N_f = 2 + 1$ and $N_f = 3$ flavors, for different values of the current quark mass am_c (in dimensionless lattice units) and volume sizes $L^3 \times 1/T$ (in units of the lattice spacing a).

may be present. In the large volume limit, we find that κ approaches its infinite-volume limit as expected. On the other hand, we find that the curvature increases rapidly for small volume sizes. This can be understood from the fact that shrinking the spatial volume of the system has a similar effect as increasing the temperature of the system which corresponds to shrinking the extent of the system in Euclidean time direction. Therefore the constituent quark mass decreases eventually with decreasing L. In turn, the system becomes more sensitive to the presence of a finite chemical potential and the curvature κ becomes bigger.

Between these two asymptotical limits of large and small volume sizes, the shape of the curvature $\kappa(L)$ as a function of the volume size depends on the choice of the boundary conditions for the quarks in spatial directions as well as on $m_\pi^{(0)}$. Since we are interested in a comparison with lattice simulations, where generally periodic boundary conditions are chosen, we will concentrate on this case in the following. In particular, we can define a critical volume size L_c below which $\kappa(L)$ increases, and we find that its value depends on $m_\pi^{(0)}$. We observe that L_c becomes smaller for larger values of $m_\pi^{(0)}$. In Tab. 4 we list the values of the length scale L_c, for which we take the location of the minimum in $\Delta\kappa$, for selected values of the pion mass $m_\pi(L \to \infty, T \to 0)$. In the IR regime, the value of the pion mass in infinite volume and for zero temperature provides the relevant scale. When the spatial extent of the system becomes comparable to the Compton wavelength of the pion, $L \sim 1/m_\pi^{(0)}$, the dynamics of the system become affected by the finite size of the volume. For $m_\pi^{(0)} L \ll 2\pi$, the dynamics of the theory are completely dominated by the zero modes of the fields and the curvature of the phase boundary exceeds its value in the infinite volume limit. In addition, we observe that $\kappa(L)$ has a minimum, which appears only in the case with periodic boundary conditions for the quarks in spatial directions.

The existence of such a minimum is closely related to the existence of a maximum in the constituent quark mass as a function of L for periodic boundary conditions [31]. In a constituent quark picture, the increase of the quark mass leads to a less chemical potential sensitivity of the system and hence to a decrease in the curvature. Here this manifests itself as a clear finite-volume effect.

m_π [MeV]	100	138	200
$\kappa(L \to \infty)$	1.357(18)	1.375(63)	1.409(59)

Table 3: Dependence of the curvature $\kappa(L \to \infty)$ on the pion mass $m_\pi(T = 0, L \to \infty)$. The errors result from fits of the numerical data to the transition curve with polynomials to order μ^2 , μ^4 and μ^6.

We find that the minimum of the curvature becomes deeper for a decreasing pion mass $m_\pi^{(0)}$ and for a fixed system size L. For example, the curvature deviates about 2% at its minimum at $L \simeq 3\,\mathrm{fm}$ from its infinite-volume limit for $m_\pi^{(0)} = 200\,\mathrm{MeV}$, while it deviates at the minimum almost 20% for $m_\pi^{(0)} = 100\,\mathrm{MeV}$. For $m_\pi^{(0)} \gtrsim 300\,\mathrm{MeV}$, the deviation of the curvature from its infinite volume limit is less than 1% for $L \gtrsim 2\,\mathrm{fm}$. These observations imply that an extrapolation to large volumes is rather simple and safe for large pion masses, $\kappa(L) \approx \kappa(\infty)$ for $L \gtrsim 2\,\mathrm{fm}$. However, for physical pion masses, the presence of the minimum in the curvature probably requires more elaborate extrapolation methods. In this case finite-volume effects are much more pronounced, which may have consequences for lattice QCD studies.

We would like to point out that a second extremum exists for (very) small box sizes. In our results, this is most clearly visible for $m_\pi^{(0)} = 100\,\mathrm{MeV}$, but the onset of the flattening of $\Delta\kappa$ associated with such an extremum is also visible for $m_\pi^{(0)} = 138\,\mathrm{MeV}$. The region in which significant effects can be described by our model is limited. First of all, we observe that the values of the momenta of the non-zero (spatial) momentum modes increase for decreasing volume size as

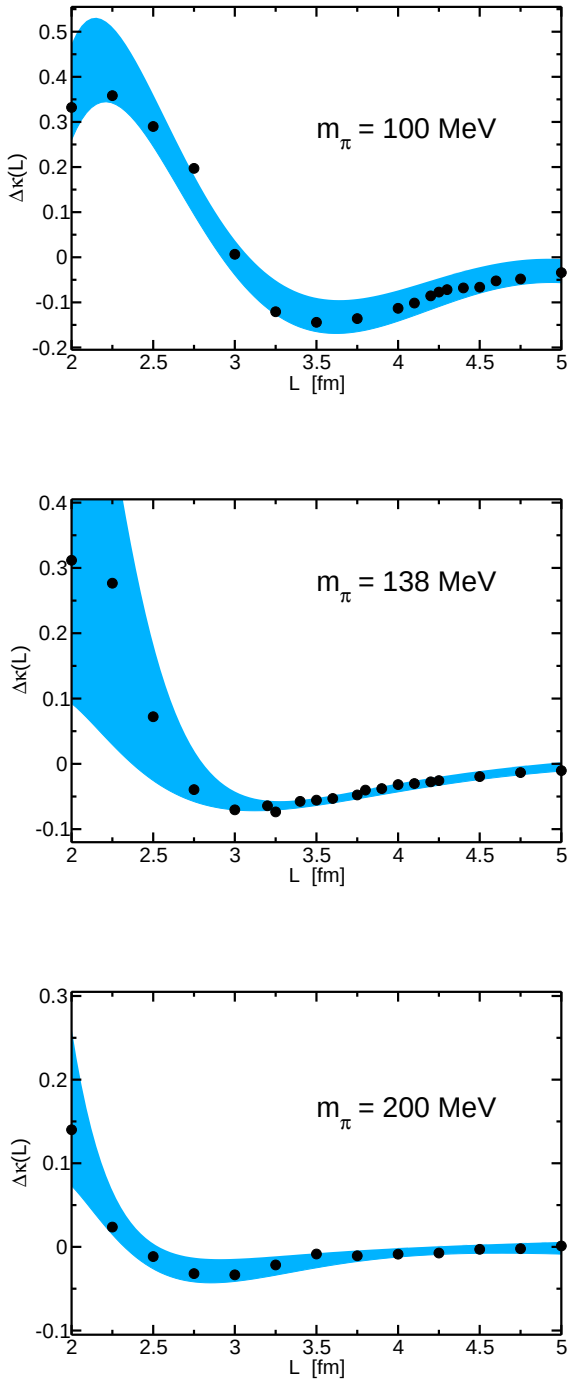

Figure 1: $\Delta\kappa(L) = (\kappa(L, m_\pi^{(0)}) - \kappa(\infty, m_\pi^{(0)}))/\kappa(\infty, m_\pi^{(0)})$ as a function of the spatial extent L of the system for various values of $m_\pi^{(0)}$. In intermediate volume ranges the curvature is reduced in comparison to its infinite-volume value. For small pion masses, the change can be as much as 20%; for a realistic value of the pion mass it is on the order of 10% and decreases further with increasing pion mass. Error bands are estimated from different fit orders (μ^2, μ^4, μ^6) to the curve $T_\chi(\mu)$.

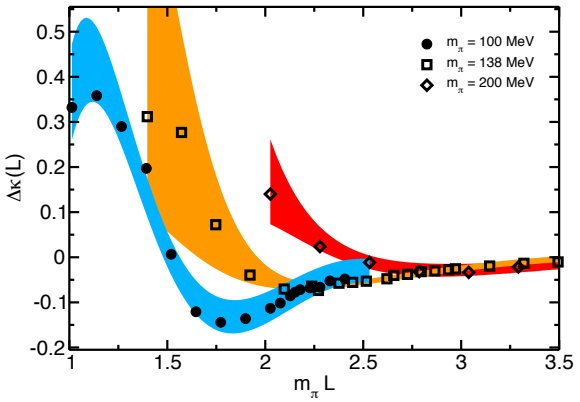

Figure 2: $\Delta\kappa(L) = (\kappa(L, m_\pi^{(0)}) - \kappa(\infty, m_\pi^{(0)}))/\kappa(\infty, m_\pi^{(0)})$ as a function of the dimensionless variable $m_\pi^{(0)} L$ of the system for all three values of $m_\pi^{(0)}$ investigated.

$1/L$. For sufficiently small volumes, we then have $2\pi/L > \Lambda$, where Λ is the UV cutoff. We expect that this small-volume regime is not accessible within our present model approach; in the same way as the high-temperature phase of QCD cannot be described accurately with our model due to the lack of gauge degrees of freedom at short length scales . Since the behavior of the curvature for (very) small volumes may very well be influenced by the fact that our model is not valid on all scales, we have to restrict ourselves to the regime with $L \gtrsim 2\pi/\Lambda \simeq 1\,\text{fm}$. Second, the length scale set by the pion mass needs to be compared to the extent of the volume. For $L \lesssim 2\pi/m_\pi^{(0)}$, the size of the box is smaller than the Compton wavelength of the pion and the partition function of the theory is dominated by the zero modes, as discussed above. Since the pion mass is the relevant scale for the low-energy dynamics, the positions of the extrema of $\Delta\kappa$ can be changed by varying the pion mass $m_\pi^{(0)}$. To be specific, the extrema are shifted to larger values of L when we decrease the pion mass $m_\pi^{(0)}$. Eventually, the constituent quark mass becomes for all practical purposes independent of L for small volume sizes, $L \ll 2\pi/m_\pi^{(0)}$, provided that we choose periodic boundary conditions for the quarks, as discussed in Ref. [31]. Therefore the chiral phase transition temperature [32] as well as the curvature remain finite and become almost independent of L in this regime.[2]

[2]The constituent quark mass tends to zero monotonically when we use antiperiodic boundary conditions in the spatial directions for the quarks [31]. In this case, the quarks do not have a spatial zero mode

In Fig. 3 we show a sketch of the chiral phase diagram for different finite volumes as obtained from our quark-meson model study. The black line denotes the crossover line in the infinite-volume limit. The black dot symbolizes the critical endpoint of the phase diagram as found in e.g. Ref. [29]. From our model study we expect that the chiral QCD phase boundary flattens for $L_c \lesssim L < \infty$. Therefore the location of a possible critical endpoint might very well be shifted to larger or smaller values of the chemical potential. For $m_\pi^{(0)} L \gg 2\pi$, the chiral phase diagram shrinks drastically both in the temperature direction as well as in the μ-direction. This means that the location of a potentially existing critical endpoint is necessarily located at small chemical potentials, see red line in Fig. 3. Since the critical length scale L_c also depends on the pion mass, this picture is overall dependent on the value of m_π.

Our present results are consistent with previous results from a proper-time renormalization group approach (PTRG), see Ref. [68]. For $L \to \infty$, the regulator in the latter study can be directly related to the regulator employed in the present work [86]. In the case of a finite volume, however, a one-to-one mapping between the PTRG flow equation and the present functional RG flow equation is not known. The qualitative agreement of our present study with the results in Ref. [68] suggests that the general behavior of the curvature as a function of the volume size is independent of the regularization scheme.

4. Conclusions and Outlook

We have used a non-perturbative functional renormalization group approach to investigate how the curvature of the chiral phase transition line close to $\mu = 0$ is affected by the volume size. We employed a quark-meson model with two flavors at finite temperature and chemical potential in a finite volume. The various parameters of this model have been fixed such that the values of the pion mass and the pion decay constant at vanishing temperature and chemical potential are consistent with chiral perturbation theory.

The curvature is accessible to lattice QCD calculations in spite of the fermion sign problem at non-vanishing chemical potential. Lattice results for the curvature obtained for different values of the quark mass and in different volume sizes differ significantly, and it appears worthwhile to investigate volume effects.

and the curvature tends to zero for small volumes sizes, $1/L \gg \mu$, see Ref. [70].

m_π [MeV]	100	138	200
L_c [fm]	3.64(2)	3.19(8)	2.97(22)
$m_\pi^{(0)} L_c$	1.84(1)	2.23(6)	3.01(22)
$\Delta\kappa(L_c)$	−0.14(2)	−0.067(5)	−0.025(13)

Table 4: Critical length scale L_c at which the curvature has a minimum. Results are given for three different values of the infinite-volume pion mass $m_\pi(T = 0, L \to \infty)$. To find the minimum, one needs to explore the region where the dimensionless quantity $m_\pi^{(0)} L_c \approx 2 - 3$. The errors result from fits of the numerical data to the transition curve with polynomials to order μ^2 , μ^4 and μ^6.

We find a qualitatively clear picture for the behavior of the curvature in a finite volume. With periodic boundary conditions for the quark fields in the spatial directions, as done in many lattice calculations, the curvature decreases in intermediate volumes, and the observed curvature is smaller than in the infinite-volume limit. Below a certain critical length scale, which depends on the value of the infinite-volume pion mass, the curvature again increases strongly.

We interpret these results in terms of a constituent quark picture: An increasing constituent quark mass makes the system less sensitive to a change in the chemical potential and leads to a decrease in the curvature. For periodic spatial boundary conditions for the quark fields, such an effect has been observed in RG quark-meson model studies. For small volume sizes, similar to the behavior at finite temperature, chiral symmetry tends to be restored and the constituent quark mass decreases rapidly which finally leads to a strong increase in the curvature.

While the pion mass dependence of the chiral transition temperature, obtained from the model, is stronger than the one observed in calculations including gauge degrees of freedom, the pion mass dependence of the observed change in the curvature is more closely related to the infrared (long-range) physics of the system and hence likely less dependent on microscopic details of the model.

In the present study, we have found that the dependence of the curvature on the volume size is weak for larger pion masses. Our results suggest that this dependence becomes increasingly larger when realistic pion masses are approached in QCD lattice simulations. The observed effect would lead to a flattening of the chiral phase transition line in the QCD phase diagram for small values of μ in an intermediate volume range. As a consequence, in this volume range the location of a possible critical endpoint could well be shifted. For small volumes, the region with broken chiral symmetry shrinks dramatically, and a possible critical endpoint

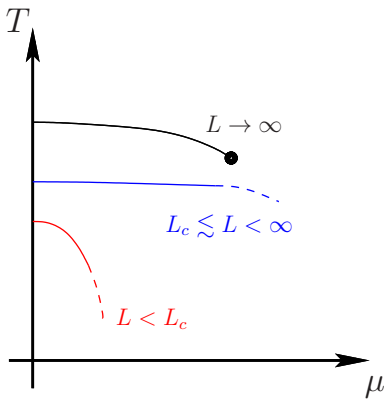

Figure 3: Sketch of the QCD phase diagram for small chemical potentials for different volume sizes L. The straight lines symbolize the chiral crossover line. The black dot symbolizes the critical endpoint of the chiral phase diagram from a quark-meson model study, e.g. [29].

would be shifted to small values of the chemical potential. Studies in this direction are ongoing and will be published elsewhere [70].

It is interesting to speculate whether the confining dynamics in the gauge sector alter the present results qualitatively. This is of course an important question in gauging the validity of the current results and relevant to making contact with lattice simulations on a quantitative level. In order to better understand how confining dynamics change our results for the curvature, one may include the Polyakov loop in the present study along the lines of Refs. [87, 88] and as shown in Appendix A. The associated corrections leave the zero-temperature dynamics unchanged. At finite temperature, however, the quarks are effectively screened due to their coupling to the confinement order parameter. We expect that the inclusion of this special type of gauge dynamics will yield only a quantitative change of the volume dependence of the curvature. The qualitative behavior of the curvature as a function of the box size likely persists. A detailed study of this conjecture also requires the inclusion of finite-volume effects in the gauge sector (see, e. g., Refs. [92, 93, 94]) and is therefore deferred to future work.

Finally, we would like to emphasize that our present study is primarily meant to show that the chiral QCD phase boundary may have an intriguing dependence on the volume size. At the present stage, a quantitative comparison of the absolute values for the curvature with the ones found in lattice simulations is difficult. In fact, the absolute value of the curvature is not the heart of the present study, but rather an interest in the change of the curvature when the volume of the system is varied. In this respect, our investigation shows that there is a qualitative effect which can lead to smaller curvatures κ in a finite volume when compared to larger or infinite volumes. This could also partly account for differences in the curvature observed in QCD lattice simulations in differently sized volumes and help to guide future lattice studies of this quantity.

– *Acknowledgments* – The authors are very grateful to H. Gies and J. M. Pawlowski for useful discussions. JB acknowledges financial support by the DFG under Grant BR 4005/2-1 and the DFG research training group GRK 1523/1. Moreover, this work was partly supported by the Natural Sciences and Engineering Research Council of Canada (NSERC). TRIUMF receives federal funding via a contribution agreement through the National Research Council of Canada. BK acknowledges support of the DFG research cluster "Structure and Origin of the Universe". In addition, this work was supported by the Helmholtz-University Young Investigator Grant No. VH-NG-332.

Appendix A. Chiral Order-Parameter Potential and the Polyakov Loop

For illustration purposes, we show the flow equation for the effective (order-parameter) potential U in the limit of vanishing quark chemical potential. It is a straightforward generalization of Eq. (8) and reads

$$\begin{aligned}\partial_t U_k(\phi^2) \;=\; & k^5\Bigg[\frac{3}{E_\pi}\left(\frac{1}{2}+n_B(E_\pi)\right)\mathcal{B}_{\rm p}(kL) \\ & +\frac{1}{E_\sigma}\left(\frac{1}{2}+n_B(E_\sigma)\right)\mathcal{B}_{\rm p}(kL) \\ & -\frac{2N_f}{E_q}\sum_{j=1}^{N_{\rm c}}\Big(1-n_F(E_q,-{\rm i}\bar{g}\langle A_0\rangle_j) \\ & -n_F(E_q,{\rm i}\bar{g}\langle A_0\rangle_j)\Big)\mathcal{B}_1(kL)\Bigg],\end{aligned}$$

where $\langle A_0\rangle$ represents the minimum of the Polyakov-loop potential, i. e. the order-parameter potential for confinement [89, 90, 91]. The sum runs over the eigenvalues of the gluonic background field $\langle A_0^a\rangle T^a$. The T^a denote the generators of the underlying SU($N_{\rm c}$) gauge group in the fundamental representation. Of course, this flow equation can be generalized to finite quark chemical potential and can also be rewritten such that it depends directly on the Polyakov-loop $\langle {\rm tr}_{\rm F} L[A_0]\rangle = \langle {\rm tr}_{\rm F}\mathcal{P}\exp({\rm i}\bar{g}\int_0^{1/T} dx_0 A_0)\rangle/N_{\rm c}$ by assuming [39] that $\langle {\rm tr}_{\rm F} L[A_0]\rangle = {\rm tr}_{\rm F} L[\langle A_0\rangle]$ as well as $N_{\rm c}^n {\rm tr}_{\rm F}(L[\langle A_0\rangle])^n = N_{\rm c}({\rm tr}_{\rm F} L[\langle A_0\rangle])^n$ with $n \in \mathbb{N}$, see Refs. [50, 51, 52].

References

[1] Z. Fodor and S. D. Katz, JHEP **04**, 050 (2004), hep-lat/0402006.
[2] Z. Fodor and S. D. Katz, Phys. Lett. **B534**, 87 (2002), hep-lat/0104001.
[3] Z. Fodor and S. D. Katz, JHEP **03**, 014 (2002), hep-lat/0106002.
[4] Z. Fodor, S. D. Katz, and K. K. Szabo, Phys. Lett. **B568**, 73 (2003), hep-lat/0208078.
[5] C. Allton *et al.*, Phys.Rev. **D66**, 074507 (2002), hep-lat/0204010.
[6] C. R. Allton *et al.*, Phys. Rev. **D68**, 014507 (2003), hep-lat/0305007.
[7] C. R. Allton *et al.*, Phys. Rev. **D71**, 054508 (2005).
[8] R. V. Gavai and S. Gupta, Phys.Rev. **D68**, 034506 (2003), hep-lat/0303013.
[9] R. Gavai and S. Gupta, Phys.Rev. **D71**, 114014 (2005), hep-lat/0412035.
[10] R. Gavai and S. Gupta, Phys.Rev. **D78**, 114503 (2008), 0806.2233.
[11] P. de Forcrand and O. Philipsen, Nucl. Phys. **B642**, 290 (2002), hep-lat/0205016.
[12] P. de Forcrand and O. Philipsen, Nucl. Phys. Proc. Suppl. **119**, 535 (2003), hep-lat/0209084.
[13] P. de Forcrand and O. Philipsen, (2003), hep-ph/0301209.
[14] M. Wagner, A. Walther, and B.-J. Schaefer, Comput. Phys. Commun. **181**, 756 (2010), 0912.2208.
[15] F. Karsch, B.-J. Schaefer, M. Wagner, and J. Wambach, Phys.Lett. **B698**, 256 (2011), 1009.5211.
[16] O. Philipsen, PoS **LAT2005**, 016 (2006), hep-lat/0510077.
[17] C. Schmidt, PoS **LAT2006**, 021 (2006), hep-lat/0610116.
[18] O. Philipsen, Prog.Theor.Phys.Suppl. **174**, 206 (2008).
[19] P. de Forcrand, PoS **LAT2009**, 010 (2009), 1005.0539.
[20] P. de Forcrand and O. Philipsen, JHEP **01**, 077 (2007).
[21] F. Karsch *et al.*, Nucl. Phys. Proc. Suppl. **129**, 614 (2004), hep-lat/0309116.
[22] O. Kaczmarek *et al.*, Phys.Rev. **D83**, 014504 (2011).
[23] G. Endrodi, Z. Fodor, S. Katz, and K. Szabo, JHEP **1104**, 001 (2011), 1102.1356.
[24] D. Jungnickel and C. Wetterich, Eur.Phys.J. **C1**, 669 (1998), hep-ph/9606483.
[25] D. Jungnickel and C. Wetterich, Phys.Rev. **D53**, 5142 (1996), hep-ph/9505267.
[26] J. Berges, D. U. Jungnickel, and C. Wetterich, Phys. Rev. **D59**, 034010 (1999), hep-ph/9705474.
[27] B.-J. Schaefer and H.-J. Pirner, Nucl. Phys. **A660**, 439 (1999), nucl-th/9903003.
[28] J. Braun, K. Schwenzer, and H.-J. Pirner, Phys. Rev. **D70**, 085016 (2004), hep-ph/0312277.
[29] B.-J. Schaefer and J. Wambach, Nucl. Phys. **A757**, 479 (2005), nucl-th/0403039.
[30] J. Braun, B. Klein, and H. J. Pirner, Phys. Rev. **D71**, 014032 (2005), hep-ph/0408116.
[31] J. Braun, B. Klein, and H. J. Pirner, Phys. Rev. **D72**, 034017 (2005), hep-ph/0504127.
[32] J. Braun, B. Klein, H. J. Pirner, and A. H. Rezaeian, Phys. Rev. **D73**, 074010 (2006), hep-ph/0512274.
[33] L. M. Abreu, M. Gomes, and A. J. da Silva, Phys. Lett. **B642**, 551 (2006), hep-th/0610111.
[34] B.-J. Schaefer and J. Wambach, Phys. Rev. **D75**, 085015 (2007), hep-ph/0603256.
[35] B. Stokic, B. Friman, and K. Redlich, Eur.Phys.J. **C67**, 425 (2010), 0904.0466.
[36] L. Palhares, E. Fraga, and T. Kodama, J.Phys.G **38**, 085101 (2011), 0904.4830.
[37] L. F. Palhares and E. S. Fraga, (2011), 1107.1588.
[38] E. S. Fraga, L. F. Palhares, and P. Sorensen, Phys.Rev. **C84**, 011903 (2011), 1104.3755.
[39] P. N. Meisinger and M. C. Ogilvie, Phys.Lett. **B379**, 163 (1996), hep-lat/9512011.
[40] R. D. Pisarski, Phys.Rev. **D62**, 111501 (2000), hep-ph/0006205.
[41] A. Mocsy, F. Sannino, and K. Tuominen, Phys.Rev.Lett. **92**, 182302 (2004), hep-ph/0308135.
[42] K. Fukushima, Phys.Lett. **B591**, 277 (2004).
[43] E. Megias, E. Ruiz Arriola, and L. Salcedo, Phys.Rev. **D74**, 065005 (2006), hep-ph/0412308.
[44] C. Ratti, M. A. Thaler, and W. Weise, Phys. Rev. **D73**, 014019 (2006), hep-ph/0506234.
[45] S. Roessner, C. Ratti, and W. Weise, Phys. Rev. **D75**, 034007 (2007), hep-ph/0609281.
[46] C. Sasaki, B. Friman, and K. Redlich, Phys.Rev. **D75**, 074013 (2007), hep-ph/0611147.
[47] B.-J. Schaefer, J. M. Pawlowski, and J. Wambach, Phys. Rev. **D76**, 074023 (2007), 0704.3234.
[48] B.-J. Schaefer, M. Wagner, and J. Wambach, Phys.Rev. **D81**, 074013 (2010), 0910.5628.
[49] A. J. Mizher, M. Chernodub, and E. S. Fraga, Phys.Rev. **D82**, 105016 (2010), 1004.2712.
[50] V. Skokov, B. Stokic, B. Friman, and K. Redlich, Phys.Rev. **C82**, 015206 (2010), 1004.2665.
[51] T. K. Herbst, J. M. Pawlowski, and B.-J. Schaefer, Phys. Lett. **B696**, 58 (2011), 1008.0081.
[52] V. Skokov, B. Friman, and K. Redlich, Phys.Rev. **C83**, 054904 (2011), 1008.4570.
[53] J. Braun, S. Diehl, and M. M. Scherer, arXiv:1109.1946.
[54] C. Wetterich, Phys. Lett. **B301**, 90 (1993).
[55] D. F. Litim and J. M. Pawlowski, in *The Exact Renormalization Group*, Eds. Krasnitz et al., World Scientific , 168 (1999), hep-th/9901063.
[56] C. Bagnuls and C. Bervillier, Phys.Rept. **348**, 91 (2001), hep-th/0002034.
[57] J. Berges, N. Tetradis, and C. Wetterich, Phys.Rept. **363**, 223 (2002), hep-ph/0005122.
[58] J. Polonyi, Central Eur.J.Phys. **1**, 1 (2003), hep-th/0110026.
[59] B. Delamotte, D. Mouhanna, and M. Tissier, Phys.Rev. **B69**, 134413 (2004), cond-mat/0309101.
[60] J. M. Pawlowski, Annals Phys. **322**, 2831 (2007), hep-th/0512261.
[61] H. Gies, hep-ph/0611146.
[62] B.-J. Schaefer and J. Wambach, Phys.Part.Nucl. **39**, 1025 (2008), hep-ph/0611191.
[63] B. Delamotte, cond-mat/0702365.
[64] O. J. Rosten, arXiv:1003.1366.
[65] J. M. Pawlowski, AIP Conf. Proc. **1343**, 75-80 (2011). [arXiv:1012.5075 [hep-ph]].
[66] J. Braun, arXiv:1108.4449.
[67] J. Braun and B. Klein, Eur. Phys. J. **C63**, 443 (2009).
[68] B. Klein, J. Braun, and B.-J. Schaefer, PoS **LATTICE2010**, 193 (2010), 1011.1435.
[69] J. Braun, B. Klein, and P. Piasecki, Eur.Phys.J. **C71**, 1576 (2011), 1008.2155.
[70] R.-A. Tripolt, J. Braun, B. Klein, and B.-J. Schaefer, in preparation (2012).
[71] D. B. Carpenter, C. F. Baillie, Nucl. Phys. **B260**, 103 (1985).
[72] J. Luecker, C. S. Fischer, and R. Williams, Phys. Rev. **D81**, 094005 (2010), 0912.3686.
[73] J. Braun, Phys. Rev. **D81**, 016008 (2010), 0908.1543.
[74] J. Braun, Eur. Phys. J. **C64**, 459 (2009), 0810.1727.
[75] J. Braun, H. Gies, and D. D. Scherer, Phys.Rev. **D83**, 085012 (2011), 1011.1456.
[76] D. F. Litim and J. M. Pawlowski, JHEP **11**, 026 (2006), hep-

th/0609122.
[77] J.-P. Blaizot, A. Ipp, R. Mendez-Galain, and N. Wschebor, Nucl. Phys. **A784**, 376 (2007), hep-ph/0610004.
[78] D. F. Litim, Phys. Lett. **B486**, 92 (2000), hep-th/0005245.
[79] D. F. Litim, Phys. Rev. **D64**, 105007 (2001), hep-th/0103195.
[80] D. F. Litim, Int.J.Mod.Phys. **A16**, 2081 (2001), hep-th/0104221.
[81] N. Tetradis and C. Wetterich, Nucl. Phys. **B422**, 541 (1994), hep-ph/9308214.
[82] G. Papp, B. J. Schaefer, H. J. Pirner, and J. Wambach, Phys. Rev. **D61**, 096002 (2000), hep-ph/9909246.
[83] G. Colangelo and S. Durr, Eur.Phys.J. **C33**, 543 (2004), hep-lat/0311023.
[84] D. Toublan, Phys. Lett. **B621**, 145 (2005).
[85] F. Karsch, E. Laermann, and A. Peikert, Nucl. Phys. **B605**, 579 (2001), hep-lat/0012023.
[86] D. F. Litim and J. M. Pawlowski, Phys. Lett. **B516**, 197 (2001), hep-th/0107020.
[87] J. Braun, L. M. Haas, F. Marhauser, and J. M. Pawlowski, Phys.Rev.Lett. **106**, 022002 (2011).
[88] J. Braun and A. Janot, arXiv:1102.4841.
[89] J. Braun, H. Gies, and J. M. Pawlowski, Phys.Lett. **B684**, 262 (2010), 0708.2413.
[90] F. Marhauser and J. M. Pawlowski, arXiv:0812.1144.
[91] J. Braun, A. Eichhorn, H. Gies, and J. M. Pawlowski, Eur.Phys.J. **C70**, 689 (2010), 1007.2619.
[92] A. Bazavov, B. A. Berg, Phys. Rev. **D76**, 014502 (2007). [hep-lat/0701007].
[93] C. S. Fischer, A. Maas, J. M. Pawlowski, L. von Smekal, Annals Phys. **322**, 2916-2944 (2007). [hep-ph/0701050].
[94] B. A. Berg, H. Wu, arXiv:1109.0599 [hep-lat].